

## Supporting Information

### **Enhanced photothermal performance of graphene oxide by perylene diimide radical anions / $\alpha$ -phenylethylamine hydrogen bonded complex embedded in graphene oxide films for solar water evaporation**

*Yuanyuan Li<sup>a</sup>, Jinming Liu<sup>a</sup>, Wei Li<sup>a</sup>, Yingru Li<sup>b</sup>, Wei Zhao<sup>b</sup>, Haiquan Zhang<sup>a,c,\*</sup>*

*<sup>a</sup> State Key Laboratory of Metastable Materials Science and Technology, Yanshan University, Qinhuangdao 066004, P. R. China*

*<sup>b</sup> College of Intelligent Systems Science and Engineering, Hubei Minzu University, 445000, P. R. China*

*<sup>c</sup> State Key Laboratory of Luminescent Materials and Devices, South China University of Technology, Guangzhou 510640, P. R. China*

*\*Corresponding author.*

*E-mail address: [hqzhang@ysu.edu.cn](mailto:hqzhang@ysu.edu.cn) (Haiquan Zhang)*

## 1. Determination of specific surface area

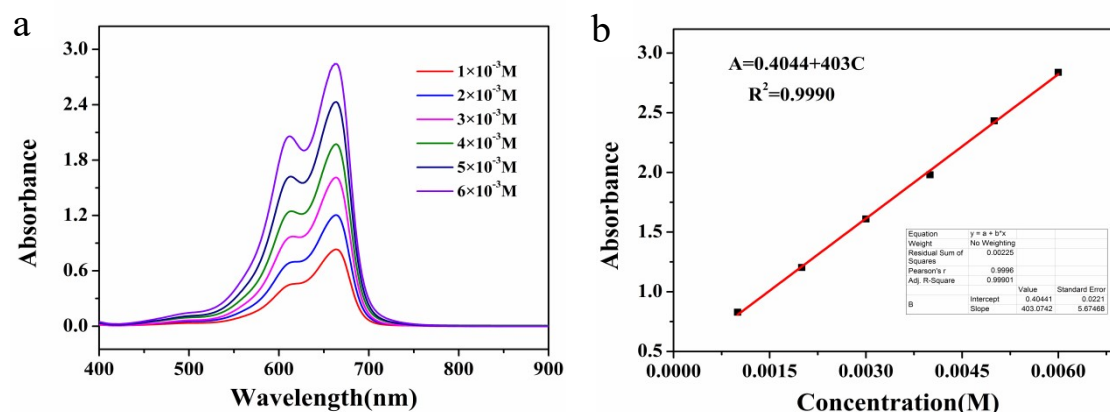


Figure S1. (a) UV-Vis spectra of aqueous solutions of methylene blue at different concentrations.

(b) Standard concentration curve of methylene blue aqueous solution.

The solution adsorption method was used to determine and compare the specific surface area of GO films and  $\alpha$ -PEA-PDI-/GO films[1-3]. First, different concentrations of aqueous methylene blue solutions were configured and their UV spectra were measured as shown in Figure S1a. Then the standard concentration curves of aqueous methylene blue solutions were plotted according to the absorbance at 664 nm as shown in Figure S1b. Then the sample bottles 1 containing 5 mg of GO film and 10 mg of  $\alpha$ -PEA-PDI-/GO film were added to 5 mL of methylene blue solution with a concentration of  $5.1 \times 10^{-3}$  M. The sample vial 1 and 2 were fully shaken in an ultrasonic shaking water bath for 2 h. After standing, the filtrate was taken and the UV spectra were measured as shown in Figure S2, and the concentrations of aqueous methylene blue solution in sample vials 1 and 2 after shaking and adsorption were calculated as  $1.99 \times 10^{-3}$  M and  $9.1 \times 10^{-4}$  M, respectively, according to the standard curve in Figure S1b. The specific surface area of the GO film and  $\alpha$ -PEA-PDI-/GO film were calculated according to the following equation:

$$S = \Gamma^{\infty} N_A A / \Gamma M$$

$M$  is the molecular weight of the adsorbent (methylene blue),  $N_A$  is the Avogadro's constant,  $\Gamma$  is the mass of the adsorbent (GO film or  $\alpha$ -PEA-PDI-/GO film),  $\Gamma^{\infty}$  is the mass of the adsorbent when the adsorption reaches saturation, and  $A$  is

the projected area of adsorbed molecules of the adsorbent.

By reviewing the literature, the specific surface area of graphene oxide in aqueous solution is about  $736.6 \text{ m}^2/\text{g}$ [4], which is brought into the above equation to obtain  $\Gamma^\infty$  of  $3.912 \times 10^{-17} \text{ \AA}^2$ , and finally  $\alpha\text{-PEA}\cdots\text{PDI}^-/\text{GO}$  film has a specific surface area of about  $986.96 \text{ m}^2/\text{g}$ , but the specific surface area of the graphene oxide film is nearly 22.32 times smaller compared to that in aqueous solution due to the stacking effect under solid state conditions[5], so the final determination of the GO film and  $\alpha\text{-PEA}\cdots\text{PDI}^-/\text{GO}$  films with specific surface areas of  $33 \text{ m}^2/\text{g}$  and  $44.2 \text{ m}^2/\text{g}$ , respectively.

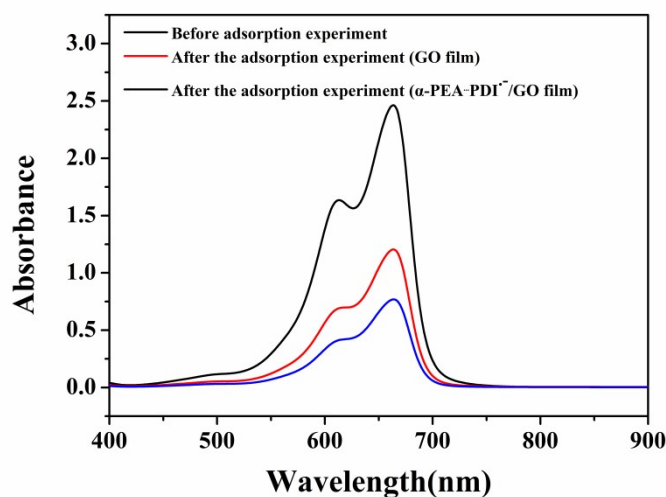


Figure S2. Changes in UV-Vis spectra of aqueous methylene blue solutions before and after adsorption.

## 2. Structural characterization

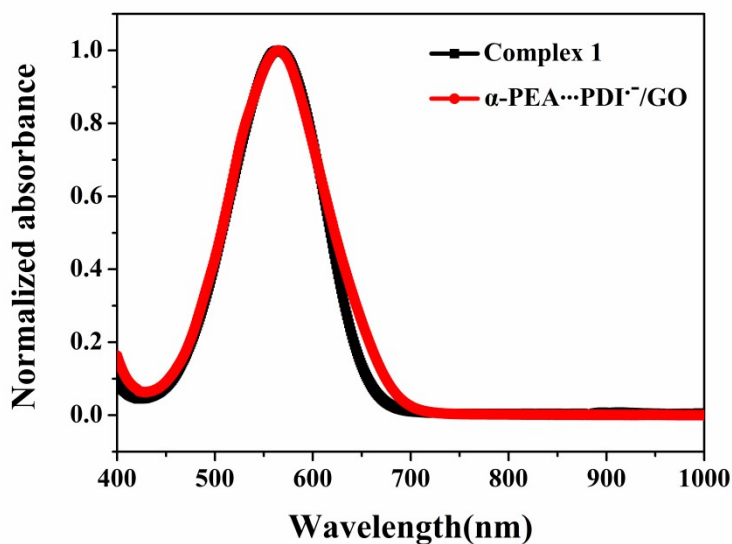


Figure S3. UV-Vis spectra of  $\alpha$ -PEA $\cdots$ PDI $^{-}$  and **1** from previous work [1] in DCM.

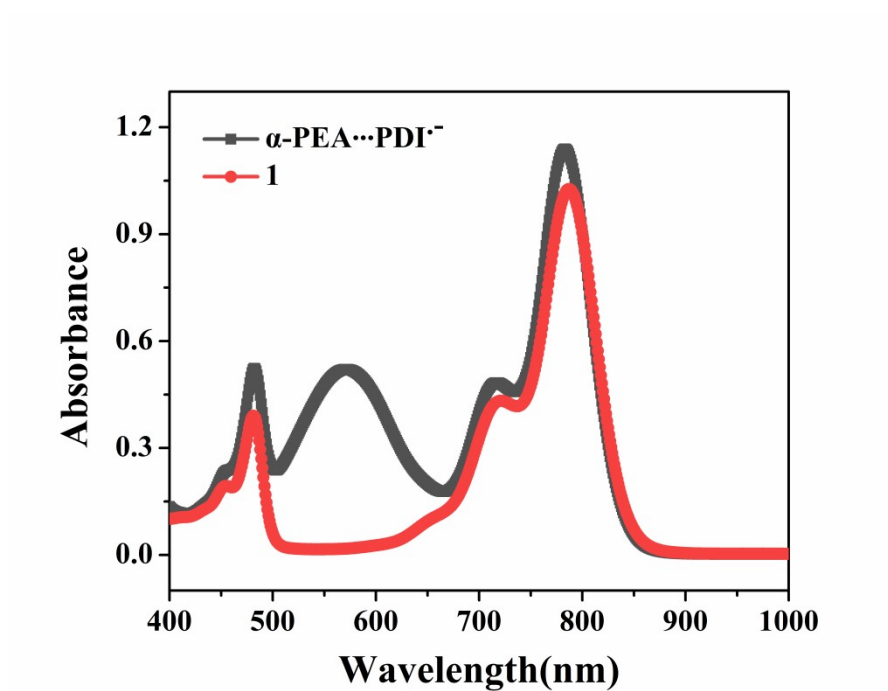


Figure S4. UV-Vis spectra of  $\alpha$ -PEA $\cdots$ PDI $^{-}$  and **1** from previous work [2] in DMF.

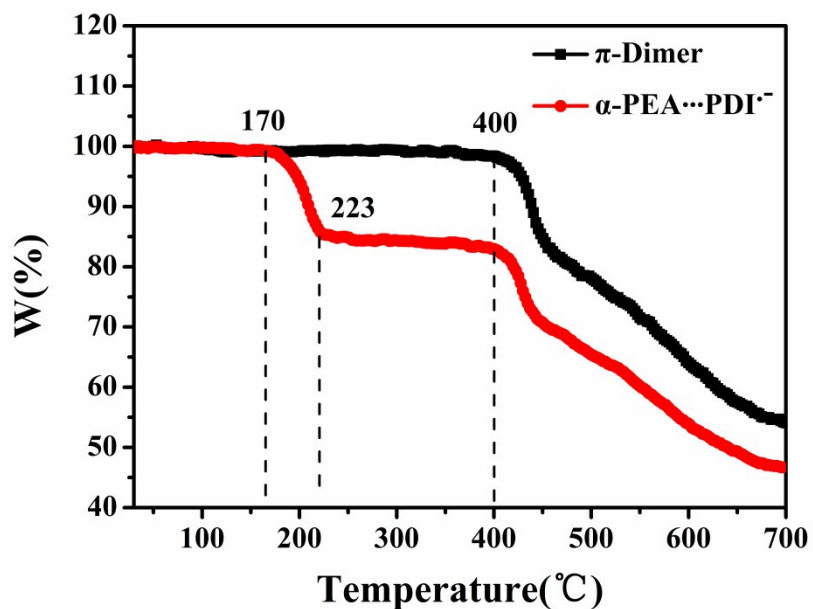


Figure S5. Thermogravimetric curves of  $\pi$ -dimer and  $\alpha$ -PEA $\cdots$ PDI $^{-}$ .

The maximum absorption peak of the UV-Vis spectra of  $\alpha$ -PEA $\cdots$ PDI $^{-}$  dissolved in DCM (shown in Fig. S1) appeared at 564 nm, which is same as the maximum

absorption peak of complex **1** in DCM solvent in the previous work[6]. The maximum absorption peak of the UV-Vis spectrum of  $\alpha$ -PEA $\cdots$ PDI $^-$  dissolved in DMF (shown in Fig. S2) appeared at 784 nm, which is almost the same as the maximum absorption peak of **1** in DMF solvent (787 nm) in the previous work in terms of peak shape and peak position, and the absorption peaks at 481 nm are the same in both shape and peak position. The only difference is that  $\alpha$ -PEA $\cdots$ PDI $^-$  shows a characteristic absorption peak at 570 nm, which in previous work **1** can only be seen in aqueous solution as a free radical aggregate, and the peak position is significantly blue-shifted, and the appearance of this peak can provide a driving force for the photothermal conversion process[7]. This not only indicates that the structure of  $\alpha$ -PEA $\cdots$ PDI $^-$  is the same as **1** (as shown in Scheme 1), but also shows that the number of radical groups contained in  $\alpha$ -PEA $\cdots$ PDI $^-$  is larger and the number of radical aggregates is more, which can provide more conversion power than **1** in the photothermal conversion process, which is consistent with the experimental results in Figure 2. Not only that, the thermogravimetric curve in Figure S2 shows the existence of two decomposition temperatures for the decomposition process of  $\alpha$ -PEA $\cdots$ PDI $^-$ , which are 170°C and 400° C, respectively. After calculation, the weight loss of the first decomposition process located at 170°C and 223°C is exactly the weight of one  $\alpha$ -phenylethylamine molecule, and the second decomposition process occurring at 400°C is almost the same as the decomposition process of  $\pi$ -dimer in the previous work, which indicates that  $\alpha$ -PEA $\cdots$ PDI $^-$  achieves the organic combination of  $\alpha$ -phenylethylamine and  $\pi$ -dimer, further proving the structure in Scheme 1 correctness.

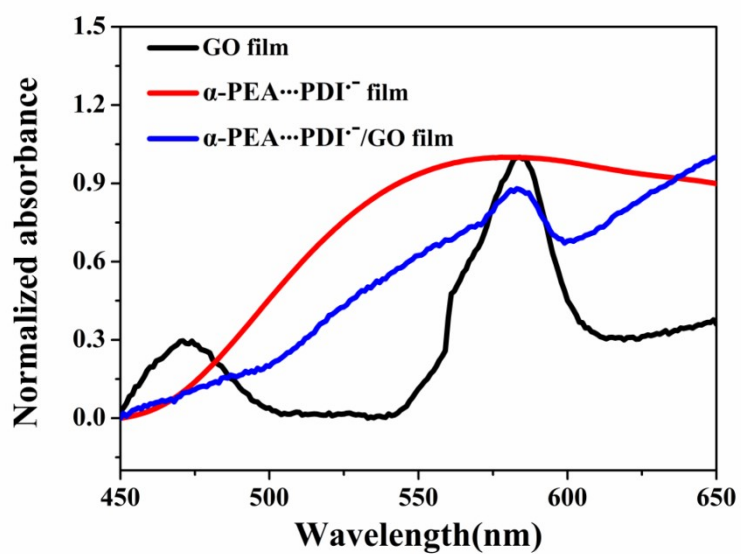


Figure S6. The solid UV-Vis spectra of GO film and  $\alpha$ -PEA/PDI/GO film.

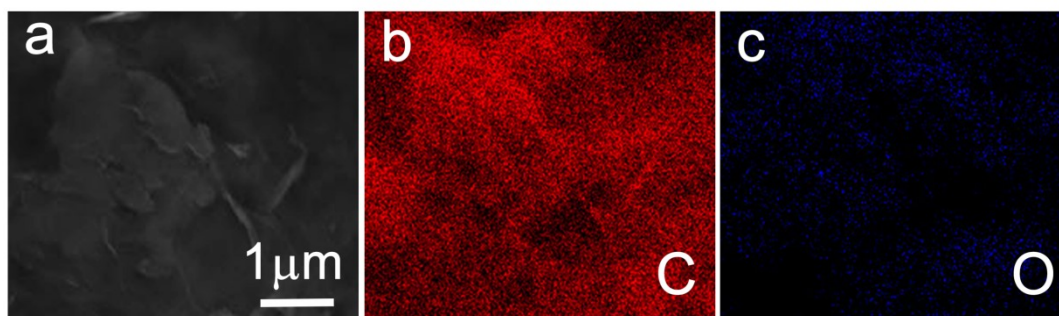


Figure S7. EDX-mapping images of C and O elements in GO film.

Table S1. The specific parameters of the EDX-mapping.

Elt.	Line	Intensity (c/s)	Atomic %	Atomic Ratio	Conc	Units	Error 2-sig	MDL 3-sig	
C	Ka	381.93	50.852	1.0347	43.717	wt.%	0.606	0.278	
N	Ka	0.00	0.000	0.0000	0.000	wt.%	0.000	0.000	
O	Ka	243.11	49.148	1.0000	56.283	wt.%	0.957	0.334	
F	Ka	0.00	0.000	0.0000	0.000	wt.%	0.000	0.000	
			100.000		100.000	wt.%			Total

### 3. The stability comparison of perylene diimide radical anion and perylene diimide radical anions/n-butylamine hydrogen bonded

## complex[6].

It is well known that the stability of perylene diimide radical anion is extremely poor and they are highly susceptible to reduction to the native state in oxygen, so the preparation of perylene diimide radical anion is always a challenge, but the UV-Vis spectra of the hydrogen-bonded complex we prepared by introducing alkyl primary amines with perylene diimide radical anion showed almost no change under the heating condition of 100 °C and only slight change in the UV-Vis spectra after one week in air, which indicates that the perylene diimide radical anion/alkyl primary amine hydrogen-bonded complex have good thermal stability and air stability compared to perylene diimide radical anion.

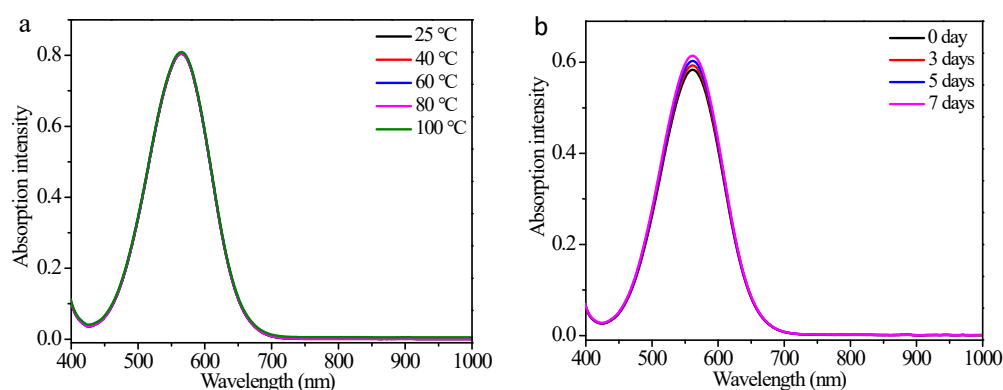


Figure S8. (a) Thermal stability of the perylene diimide radical anions/n-butylamine hydrogen bonded complex. (b) Air stability of the perylene diimide radical anions/n-butylamine hydrogen bonded complex.

#### 4. Detailed derivation and calculation of photothermal conversion efficiency for $\alpha$ -PEA-PDI-/GO film.

The photothermal conversion efficiency of  $\alpha$ -PEA-PDI-/GO film could be calculated from the energy balance during the irradiation[8]. Detailed calculation was given as following:

$$\sum_i m_i C_{p,i} \frac{dT}{dt} = Q_s + Q_{loss} \quad (1)$$

where  $m_i$  (10.2mg) and  $C_{p,i}$  (1.4J/(g $^{\circ}$ C)) are the mass and heat capacity of system components (cocrystal samples and substrate), respectively.  $Q_s$  is the photothermal energy input by irradiating Xe lamp laser to  $\alpha$ -PEA-PDI-/GO film, and  $Q_{loss}$  is thermal energy lost to the surroundings. When the temperature is maximum, the system is in balance. (2)

$$Q_s = Q_{loss} = hA(T_{max} - T_{surr}) = hA\Delta T_{max}$$

where  $h$  is the heat transfer coefficient,  $A$  is the irradiated area of the container and  $T_{surr}$  is the temperature of surrounding (can be regarded as constant).  $T_{max}$  is the maximum temperature and  $\Delta T_{max}$  is the maximum temperature change.

Define the photothermal conversion efficiency  $\eta$  as the fraction of the total light energy that is converted to heat, that is: (3)

$$\eta = \frac{hA\Delta T_{max}}{I(1 - 10^{-A_{808}})}$$

where  $I$  is the laser power (100mW/cm $^2$ ) and  $A_{808}$  is the absorbance of the samples at the wavelength of 808nm (0.4285).

In order to get the  $hA$ , a dimensionless driving force temperature,  $\theta$  is introduced as follows:

$$\theta = \frac{T - T_{surr}}{T_{max} - T_{surr}}$$



A characteristic rate constant has been defined as  $\tau_s = \sum_i m_i C_{p,i} / hA$ , the al (4)

differential equation can be solved:

$$\frac{d\theta}{dt} = \frac{1}{\tau_s} \frac{Q_s}{hA\Delta T_{\max}} - \frac{\theta}{\tau_s} \quad (5)$$

When the laser is off,  $Q_s=0$ , therefore  $\frac{d\theta}{dt} = -\frac{\theta}{\tau_s}$ , and  $t = -\tau_s \ln\theta$ .

So  $hA$  could be calculated from the slope of cooling time vs  $\ln\theta$ . Therefore,  $\tau_s$  is 49 s (Figure S8) and the photothermal conversion efficiency  $\eta$  is 24.07%.

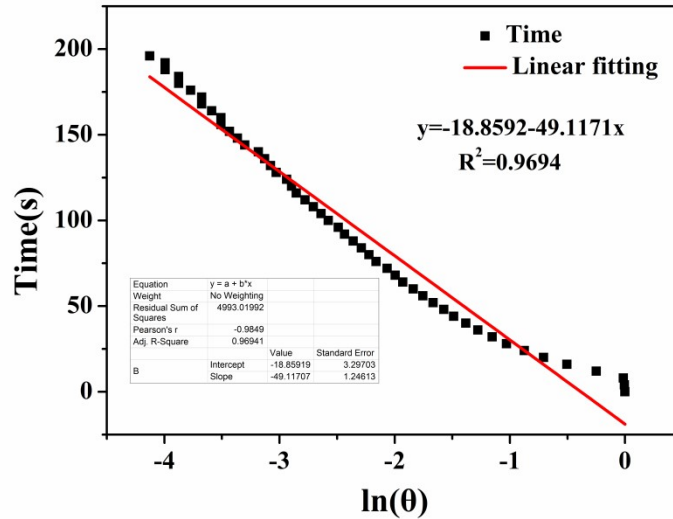


Figure S9. The calculation of the value of  $hA$  by linear fitting of temperature driving force  $\theta$  to the irradiation time  $t$  for the  $\alpha$ -PEA-PDI-GO film.

## 5. Calculation method of light absorption rate

According to the literature[9], Absorbance = 100% - Reflectance - Transmittance. Therefore, the transmission and reflection spectra of  $\alpha$ -PEA-PDI, GO film and  $\alpha$ -PEA-PDI-GO film were measured using a UV-Vis spectrophotometer as shown in the

Figure S9-S10, and the light absorption rate of  $\alpha$ -PEA-PDI<sup>-</sup>, GO film and  $\alpha$ -PEA-PDI<sup>-</sup>/GO film were calculated according to the above formula as shown in the Table S2.

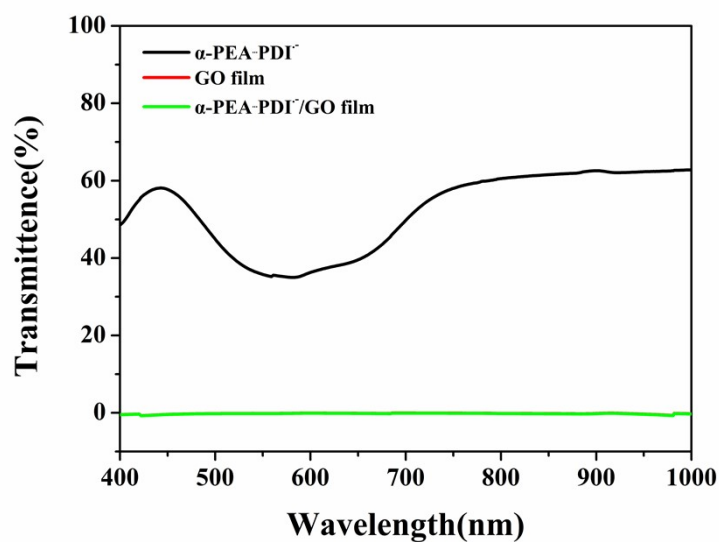


Figure S10. The transmission spectra of  $\alpha$ -PEA-PDI<sup>-</sup>, GO film and  $\alpha$ -PEA-PDI<sup>-</sup>/GO film.

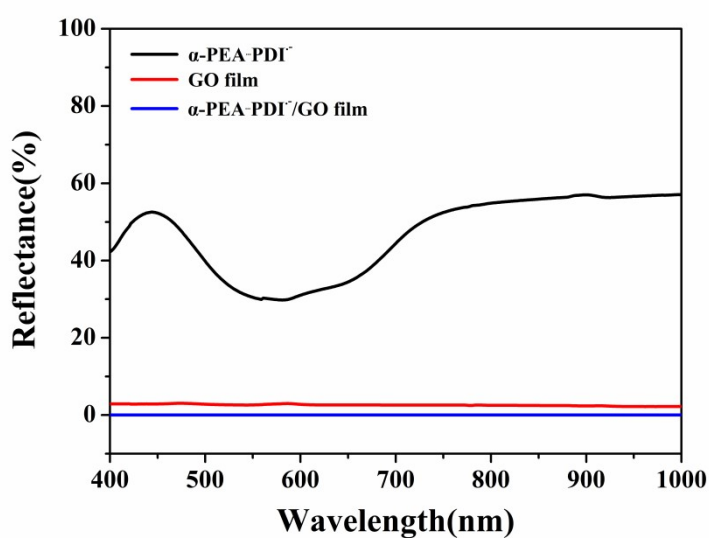


Figure S11. The reflection spectra of  $\alpha$ -PEA-PDI<sup>-</sup>, GO film and  $\alpha$ -PEA-PDI<sup>-</sup>/GO film.

Table S2. The the light absorption rate

	Average transmittance(%)	Average Reflectance(%)	light absorption rate(%)
$\alpha$ -PEA-PDI <sup>-</sup>	52.1477	46.6874	1.1649

GO film	0.0095	2.5866	97.6039
$\alpha$ -PEA-PDI-/GO film	0.0505	0.0077	99.9418

## Notes and Reference

1. Fleischfresser, B.E. and G.N. Freeland, *Measurement of external specific surface area of fibers by solution adsorption*. Journal of Applied Polymer Science, 1976. **20**(12): p. 3453-3456.
2. Giles, C.H. and S.N. Nakhwa, *Studies in adsorption. XVI The measurement of specific surface areas of finely divided solids by solution adsorption*. Journal of Applied Chemistry, 2007. **12**(6): p. 266-273.
3. Liu, N., et al., *Synthesis of functional hollow WS<sub>2</sub> particles with large surface area for Near-Infrared (NIR) triggered drug delivery*. Journal of Alloys and Compounds, 2021. **875**.
4. Montes-Navajas, P., et al., *Surface area measurement of graphene oxide in aqueous solutions*. Langmuir, 2013. **29**(44): p. 13443-8.
5. Esmaeili, A. and M.H. Entezari, *Facile and fast synthesis of graphene oxide nanosheets via bath ultrasonic irradiation*. J Colloid Interface Sci, 2014. **432**: p. 19-25.
6. Sun, M., et al., *Stable perylene diimide radical/alkylamine complex linked by asymmetric [CO...H...N]-1 -type strong H-bond and its color switching properties*. Dyes and Pigments, 2023. **209**: p. 110934.
7. Li, Y., et al., *Asymmetric anionic [O...H...N]-1 -type strong H-bond constructed new near-infrared organic photothermal materials with high molar absorptivity and high amount of temperature rise*. Dyes and Pigments, 2022. **206**: p. 110649.
8. Wang, Y., et al., *Cocrystals Strategy towards Materials for Near-Infrared Photothermal Conversion and Imaging*. Angew Chem Int Ed Engl, 2018. **57**(15): p. 3963-3967.
9. Cheng, P. and D. Wang, *Easily Repairable and High-Performance Carbon*

*Nanostructure Absorber for Solar Photothermoelectric Conversion and Photothermal Water Evaporation.* ACS Appl Mater Interfaces, 2023. **15**(6): p. 8761-8769.